MODELING STREAMS AND HYDROGEOMORPHIC ATTRIBUTES IN OREGON FROM DIGITAL AND FIELD DATA[1]

Sharon E. Clarke, Kelly M. Burnett, and Daniel J. Miller[2]

ABSTRACT: Managers, regulators, and researchers of aquatic ecosystems are increasingly pressed to consider large areas. However, accurate stream maps with geo-referenced attributes are uncommon over relevant spatial extents. Field inventories provide high-quality data, particularly for habitat characteristics at fine spatial resolutions (e.g., large wood), but are costly and so cover relatively small areas. Recent availability of regional digital data and Geographic Information Systems software has advanced capabilities to delineate stream networks and estimate coarse-resolution hydrogeomorphic attributes (e.g., gradient). A spatially comprehensive coverage results, but types of modeled outputs may be limited and their accuracy is typically unknown. Capitalizing on strengths in both field and regional digital data, we modeled a synthetic stream network and a variety of hydrogeomorphic attributes for the Oregon Coastal Province. The synthetic network, encompassing 96,000 km of stream, was derived from digital elevation data. We used high-resolution but spatially restricted data from field inventories and streamflow gauges to evaluate, calibrate, and interpret hydrogeomorphic attributes modeled from digital elevation and precipitation data. The attributes we chose to model (drainage area, mean annual precipitation, mean annual flow, probability of perennial flow, channel gradient, active-channel width and depth, valley-floor width, valley-width index, and valley constraint) have demonstrated value for stream research and management. For most of these attributes, field-measured, and modeled values were highly correlated, yielding confidence in the modeled outputs. The modeled stream network and attributes have been used for a variety of purposes, including mapping riparian areas, identifying headwater streams likely to transport debris flows, and characterizing the potential of streams to provide high-quality habitat for salmonids. Our framework and models can be adapted and applied to areas where the necessary field and digital data exist or can be obtained.

(KEY TERMS: rivers/streams; digital elevation models; watershed management; aquatic ecology; channel morphology; Geographic Information Systems.)

Clarke, Sharon E., Kelly M. Burnett, and Daniel J. Miller, 2008. Modeling Streams and Hydrogeomorphic Attributes in Oregon From Digital and Field Data. *Journal of the American Water Resources Association* (JAWRA) 44(2):459-477. DOI: 10.1111/j.1752-1688.2008.00175.x

[2]Respectively, Water Resource Specialist, Roaring Fork Conservancy, Basalt, Colorado; Research Fish Biologist, USDA Forest Service, Pacific Northwest Research Station, Corvallis, Oregon; and Senior Scientist, Earth Systems Institute, Seattle, Washington (E-Mail/Burnett: kmburnett@fs.fed.us).

INTRODUCTION

Although increasingly important for research and management of aquatic ecosystems, information on the location and characteristics of streams over large areas, spanning hundreds to millions of square kilometers, is often lacking. Stream maps (hydrography) have been produced with standard methods and are publicly accessible for many areas of the world (e.g., Geoscience Australia, 2003; DWAF (Department of Water Affairs and Forestry), 2006). Hydrography at cartographic scales of 1:24,000 and 1:100,000 is available for much of the continental United States (U.S.) (USGS, 2000). However, hydrography at these relatively coarse scales may not accurately reflect the spatial extent or location of streams. Because hydrographic data can vastly under represent streams in highly dissected terrain (Hansen, 2001), streams missing from standard hydrography have been mapped from contour crenulations on topographic maps or from air photos to create "enhanced" hydrography, as illustrated in Figure 1A. Such mapping is labor intensive and so is undertaken only for small
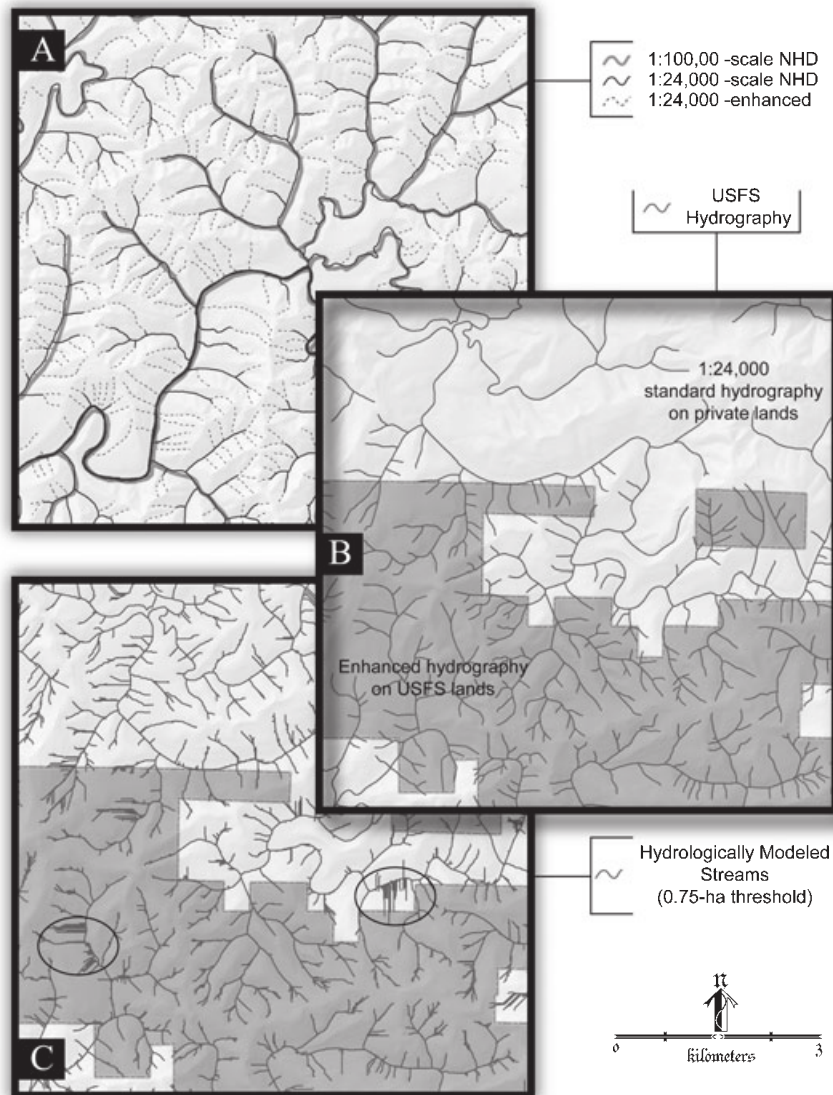

FIGURE 1. An Example Area in the Oregon Coastal Province Illustrating Issues With Standard Hydrography and With Synthetic Stream Networks. (A) Standard 1:24,000-scale and 1:100,000-scale hydrography overlaid with an enhanced stream layer, which includes streams not represented on the standard hydrography; (B) Inconsistencies in drainage density between the 1:24,000-scale hydrography as enhanced from air photos on U.S. Forest Service land and the standard hydrography available on nonfederal lands; (C) Feathering of stream channels on planar hillslopes is a problem that arises from algorithms in many software packages used to delineate stream networks from digital elevation data.

areas. Combining enhanced hydrography with standard hydrography may offer little benefit over broad areas as stream densities differ between the two data types (Figure 1B).

Public sources of hydrography typically lack basic information necessary to describe stream habitats. Fine-resolution data on stream habitat characteristics (such as pools or large wood) are commonly obtained by field inventories, using for example the methods of Hankin and Reeves (1988). Coarser-resolution data on hydrogeomorphic attributes (such as stream gradient or channel confinement), which indicate the value of habitat for lotic species (e.g., Montgomery and Buffington, 1997; Dunham et al., 2002; Burnett et al., 2007), can be obtained manually from topographic maps. Both fine-scale and coarser-scale data can be linked to hydrography in a Geographic Information Systems (GIS) (e.g., Ganio et al., 2005; Burnett et al., 2006). Manual methods to collect and link habitat data to hydrography are time consuming and costly, thus resulting outputs considered over large areas are often inconsistent or patchily distributed. Probabilistic sampling has helped satisfy the need for regionally consistent data (Stevens and Olsen, 1999; Reeves et al., 2004) but does not yield a spatially continuous description of streams.

The advent of regional digital data, together with powerful and inexpensive computers, facilitates modeling approaches in a GIS framework that can delineate synthetic hydrography and consistently estimate coarse-resolution attributes over large areas. Synthetic stream networks have been delineated from digital elevation models (DEMs) (e.g., Garbrecht and Martz, 1997; Ghizzoni et al., 2006; Lin et al., 2006) and, as illustrated in Figure 1C, can be produced with algorithms in available software packages. The spatial extent and accuracy of the results depend on numerous factors, including the resolution and quality of the DEMs, the underlying terrain, and the algorithms employed. Digital elevation data are used also to model stream attributes, including drainage area; channel gradient, sinuosity, and width; valley floors; and tributary junctions (Montgomery et al., 1998; Gallant and Dowling, 2003; Noman et al., 2003; Benda et al., 2004; Davies et al., 2007; Wondzell et al., 2007). Modeled outputs can be associated with reaches in existing hydrography or generated simultaneously with stream reaches from DEMs. Either approach can provide spatially continuous results over a relatively large area from which aquatic habitat characteristics can then be inferred. For example, Lunetta et al. (1997) derived stream gradients from 30-m DEMs to identify potential salmon habitat throughout western Washington. Field data have

been incorporated to evaluate or improve the accuracy of such DEM-derived products; however, these efforts were restricted to only one or a few stream attributes (Hemstrom et al., 2002; Noman et al., 2003; Davies et al., 2007).

Our objectives in this paper were to develop and apply methods that couple digital elevation data with higher resolution but spatially restricted field data to: (1) evaluate, calibrate, and interpret hydrogeomorphic stream attributes; (2) develop new or apply existing empirical models to estimate a larger set of attributes; and (3) delineate and evaluate a high-resolution stream network with stream attributes modeled at the reach level over a broad area. Specifically, we demonstrate for the entire Oregon Coastal Province, the use of 10-m DEMs to model a synthetic stream network along with drainage area, accumulated mean annual precipitation, mean annual flow, probability of perennial flow, channel gradient, active-channel width, active-channel depth, valley-floor width, valley-width index, and valley constraint. Such modeled stream networks can be a resource for land managers and regulators in strategic planning for large areas. The attributes reflect the capacity of streams to provide habitat and the likely response of streams to disturbance, and can be used to classify stream reach morphology (Wohl and Merrit, 2005), to explain variation in finer-scale habitat features and use by stream biota (e.g., Montgomery and Buffington, 1997; Pess et al., 2002; Roni, 2002; Wyatt, 2003), and to identify streams for different levels of riparian protection (e.g., USDA and USDI, 1994).

STUDY AREA

The Coastal Province occupies 28,873 km^2 of western Oregon (Figure 2). It is underlain primarily by marine sandstones and shales, although basaltic volcanic rocks predominate in some watersheds. Except for interior river valleys and a prominent coastal plain in a few places, the province is mountainous. Elevations range from 0 to 1250 m. Uplands are highly dissected with drainage densities up to 8.0 km/km^2 (FEMAT, 1993). Cool dry summers and mild wet winters, with heavy precipitation falling mostly from October to March, describe the climate. Potential natural vegetation is a highly productive coniferous forest consisting mainly of Douglas-fir (*Pseudotsuga menziesii*), western hemlock (*Tsuga heterophylla*), western redcedar (*Thuja plicata*), and along the coast, Sitka spruce (*Picea sitchensis*). Most of the current for-
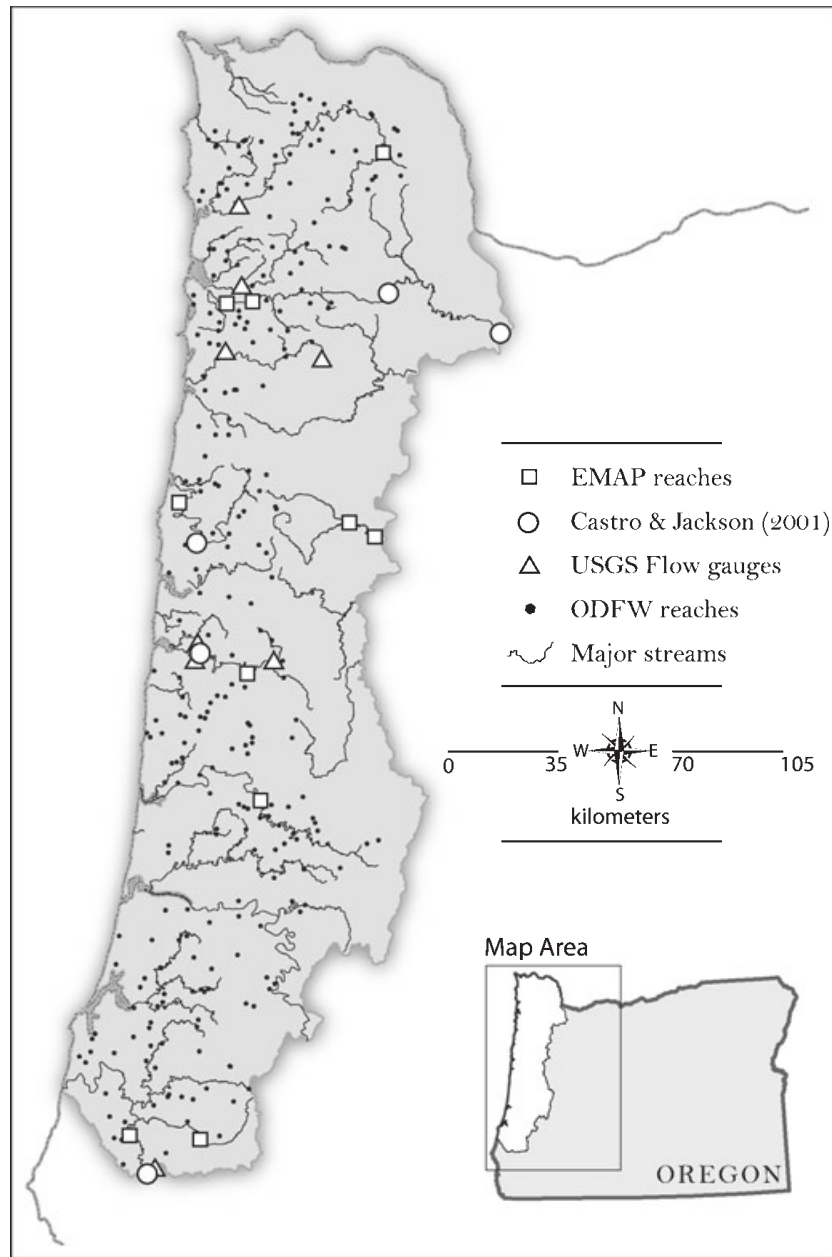
FIGURE 2. The Oregon Coastal Province With Locations of Geomorphic and Hydrologic Field Data Used in This Study.

estland is in relatively young seral stands, and the larger river valleys have been cleared for agriculture. The study area supports five salmonid species: steelhead (*Oncorhynchus mykiss*), coho salmon (*Oncorhynchus kisutch)*, cutthroat (*Oncorhynchus clarkii*), Chinook salmon (*Oncorhynchus tschawytscha*), and chum salmon (*Oncorhynchus keta*). Steelhead is listed under the U.S. ESA (1973) as a Species of Concern in the Oregon Coastal Evolutionarily Significant Unit (ESU). Coho salmon was recently relisted as a Threatened species in the Oregon Coastal ESU.

METHODS

Digital Data

We used USGS 10-m DEMs (Underwood and Crystal, 2002; Clarke and Burnett, 2003). The USGS contractor created these by interpolating elevations at DEM grid points from the digital line graph contours on 7.5-minute USGS topographic quadrangles (USGS, 1998). Streams mapped on the quadrangles (blue-line streams) were used to infer constant slope between

contours and further constrain interpolated elevations.

Mean annual precipitation (mm/year) data were from the Parameter-elevation Regressions on Independent Slopes Model (PRISM) (Water and Climate Center of the Natural Resources Conservation Service, 1998). These data were modeled using precipitation records from 1961 through 1990 and were in a 4 km resolution grid. We assigned mean annual precipitation data to each 10-m DEM cell by overlaying the PRISM grid.

Geomorphic and Hydrologic Field Data

Field data to develop the stream attributes were from six sources (Table 1 and Figure 2). The Oregon Department of Fish and Wildlife (ODF&W) supplied field-survey data from 1998 through 2001 for a variety of stream attributes (Flitcroft et al., 2002; Moore et al., 2002; ODF&W, 2007). Data were for reaches drawn from a spatially balanced, probabilistic sample of west-draining, wadeable streams depicted on 1:100,000-scale USGS topographic maps (ODF&W, 2007). Stream reaches were approximately 500-1,000 m long, and many had endpoints identified using a global positioning system (GPS). We selected the subset of reaches with both habitat surveys and estimates of juvenile salmonid abundance and included reaches with only habitat surveys when the endpoints were located with GPS. If a reach was surveyed in multiple years, we used data for the year with an annual flow that most closely approximated the mean, as determined from the nearest streamflow gauge.

The Environmental Monitoring and Assessment Program (EMAP) (Stoddard et al., 2005) supplied field data on active-channel depth and width for large streams (with drainage areas exceeding those of the ODF&W reaches (Figure 2 and Table 1). The EMAP selected sample reaches with a randomized, systematic design (Stevens and Olsen, 1999). The length of each sample reach was 40 times its low-flow wetted width. Within each sample reach, observations on active-channel depth and width were systematically located and spaced based on a randomized design (Herlihy et al., 2000).

Data supplied by the Siuslaw National Forest (SNF) were used to identify the drainage areas associated with the upper limit of perennial streamflow. Data were collected in 2002 and 2003 during late summer for selected headwater streams of the SNF. The upper limit of perennial flow was identified in the field for each stream in the dataset. This upper limit was mapped from the slope distance along the stream channel to a road/stream crossing, which allowed the point to be geo-referenced in a GIS. Drainage area boundaries were delineated, using a stereoscope with 1:12,000-scale aerial photographs, and then transferred to digital orthophotoquads to calculate drainage area.

Stream Network Delineation

Channel Initiation Criteria. Our automated extraction of the synthetic channel network from a DEM was based on algorithms that determine flow directions, calculate specific contributing area to each DEM cell, and trace channels through all cells with a contributing area exceeding some threshold value (O'Callaghan and Mark, 1984; Jenson and Domingue, 1988). Specific contributing area is contributing area per unit length of contour, or for a DEM cell, contributing area to a cell divided by the contour length crossed by flow out of the cell. Field data were lacking on the location of channel initiation sites. Therefore, as suggested by Montgomery and Foufoula-Georgiou (1993), we intended to set the channel-initiation threshold at the inflection in a plot of inferred channel densities (channel length per unit basin area) against potential threshold values. This

TABLE 1. Field Data Sources Used to Evaluate, Calibrate, Estimate, and Interpret Modeled Stream Attributes.

Source	n	Drainage Area (km^2)	Years	Stream Attributes
Oregon Department of Fish and Wildlife (ODF&W, 2007)	273	0.5-186.8	1998-2001	Drainage area, channel gradient, active-channel width, active-channel depth, valley-floor width, valley-width index, and valley constraint
Environmental Monitoring and Assessment Program (EMAP)	12	204.6-1046	1994-1998	Active-channel width and active-channel depth
Siuslaw National Forest (SNF)	123	0.0018-0.36	2002-2003	Probability of perennial flow
USGS Gauging Stations	9	16.1-1727.5	1961-1990	Drainage area and mean annual flow
Castro and Jackson (2001)	5	323.7-1828.5	1995	Active-channel depth
Federal Emergency Management Agency FEMA (1996, 1998)	124	>180	1996 and 1998	Valley-floor width

inflection indicates that channel densities increase sharply with decreasing threshold values and that delineated channels extend in profusion (feathering) onto unchannelized hillslopes (Figure 1C). However, the inflection can be indistinct and extensive feathering occurred when channels were delineated with a threshold chosen to include the upper limit of perennial flow for the SNF field-mapped points. Three modifications substantially reduced feathering: (1) we applied different thresholds for low-gradient and high-gradient areas, consistent with observations that channel initiation processes may differ for these areas (Dietrich *et al.*, 1992); (2) for low-gradient areas, we used a slope-dependent threshold, consistent with processes of channel initiation on gentle slopes (Montgomery and Foufoula-Georgiou, 1993); and (3) we incorporated a topographic convergence threshold into our criteria for channel initiation for both low-gradient and high-gradient areas.

On steep slopes in the study area, channels tend to be formed by landsliding and associated debris flows (Stock and Dietrich, 2006); on gentler slopes, channels are generally eroded by overland flow. Using field-mapped landslide locations (Robison *et al.*, 1999), we observed that no landslides initiated below DEM-derived slope gradients of 25%. For areas with gradients less than 25%, we used a slope-dependent threshold (Montgomery and Foufoula-Georgiou, 1993); the inflection in the plot of inferred channel densities against potential threshold values indicated a threshold of 16 m (Figure 3a). For slope gradients greater than 25%, we used a specific contributing area threshold with no slope dependence; the inflection in this plot of inferred channel densities against potential threshold values indicated a threshold of 360 m (Figure 3b).

To exclude channel initiation on planar hillslopes, we incorporated topographic convergence into the criteria for channel initiation. On a topographic map,

down-slope-aligned contour crenulations, indicating upward-curved topography, are associated with areas of flow concentration and presence of stream channels. Because the DEMs were interpolated from contour lines, we could use information on topographic convergence to constrain the upslope extent of channels. Topographic convergence for a DEM cell was measured as the summed proportion of each of the eight adjacent cells that flowed into it using the D∞ flow direction algorithm of Tarboton (1997). This algorithm proportions flow out of a cell into downslope cells based on slope aspect, with flow allowed into at most two downslope cells. If there is no flow into a cell (a high point), this sum is zero; if all adjacent cells flow into a cell (a single-cell pit), this sum is eight. In addition to the thresholds for channel initiation, we required a minimum flow convergence. By assessing mapped results from several potential values, we found that a convergence measure of at least 1.75 inflowing cells that persisted for at least two cells along any flow path worked well to eliminate feathering of delineated channels onto planar hillslopes.

Channel Flow Directions. Downslope dispersion was not allowed for DEM cells identified as stream channels and thus flow was directed to one of the eight adjacent cells (D-8 flow algorithm). Typical algorithms direct channelized flow along the route of steepest descent (e.g., O'Callaghan and Mark, 1984); however this sometimes produced small streams that diverged from the path indicated by contour crenulations. We found that modeled streams were better located by constraining the algorithm to direct flow to the downslope point with the largest topographic convergence, which in most but not all cases is the direction of steepest descent. For directing flow through flat areas, we used the algorithm described by Garbrecht and Martz (1997),
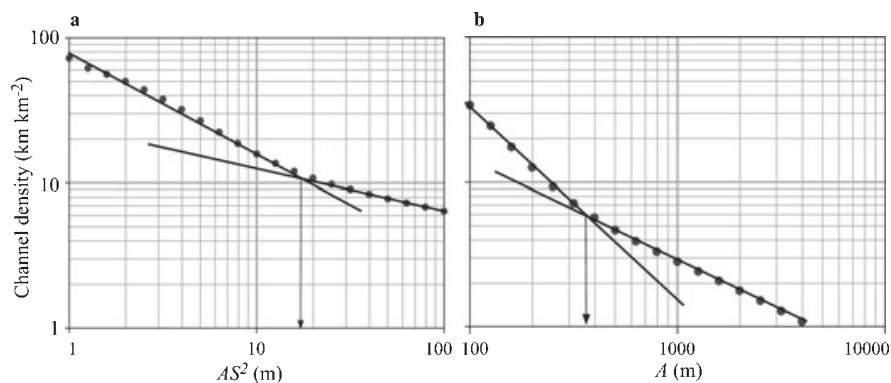

FIGURE 3. Channel Densities Plotted Against Potential Threshold Values for Initiating Stream Channels. These are based on (a) slope-dependent specific drainage area in lower gradient (<25% terrain) and (b) specific drainage area in steeper terrain.

which defines flow directions away from adjacent higher elevations and towards the lowest elevation bordering the flat zone.

The D∞ flow-direction algorithm was used to estimate the contour length crossed by flow out of each DEM cell (necessary for calculating specific contributing area). The algorithm calculates flow directions for each of the eight triangular facets defined by the center point of a cell and its eight neighbors (Tarboton, 1997). For each facet having flow out of the cell, we used the projection of flow direction on the exterior facet edge as a measure of contour length crossed by flow exiting the cell from that facet. Thus, contour length for flow perpendicular to the edge is equal to the facet edge length (one half the cell length); contour length for flow at an angle of 60° to the edge is one half the edge length; and contour length for flow parallel to or away from the edge is zero. These projection lengths are summed over all eight facets. Contour length for planar flow through a cell is one cell length, for divergent flow is more than one cell length, and for convergent flow is less than one cell length.

Stream Attributes

Stream attributes were calculated for each DEM cell in the delineated stream network. Depending upon the attribute, cell-level values were averaged over the length of a reach or assigned to a reach based on the value at the downstream-most cell. Reach-level values for the entire Oregon Coastal Province were ultimately written to a vector file in the ESRI shapefile format (ESRI, 1998). Reach breaks were placed to minimize the variance of channel gradient, valley-floor width, and drainage area in a reach while keeping lengths about 20 times the active channel width. This approximated guidance for defining reaches in the ODF&W field surveys (Moore et al., 2002).

We geo-referenced field-surveyed stream reaches (ODF&W and EMAP) and USGS streamflow gauge sites on the delineated stream network using field maps and latitude and longitude coordinates. Field-measured values for these surveyed reaches and gauge sites were compared with attribute values modeled from the DEMs.

All regression models were developed in Stat-Graphics (Version 4, 1999, StatPoint, Inc., Herndon, Virginia). Observations with unusually high studentized residuals (>3) or leverage values (>5 times the average) for a particular regression were evaluated for unusual circumstances or data collection errors, which we determined by checking field notes, the location of the reach, and other field and modeled attributes. These observations were excluded from analyses and reported degrees of freedom reflect this.

Drainage Area. This was estimated using the D∞ flow accumulation algorithm (Tarboton, 1997) for DEM cells upslope of modeled channel initiation points and using a D-8 flow algorithm (O'Callaghan and Mark, 1984) for cells downstream of these points. Drainage area (km^2) for each reach in the delineated stream network was specified as the contributing area to the downstream-most cell in the reach. To evaluate results, modeled drainage areas were regressed against mapped drainage areas determined from 7.5-minute Digital Raster Graph (DRG) data by ODF&W for the basin upstream of their field survey reaches. Values of modeled and mapped drainage areas were also regressed for reaches in the delineated stream network that contained the nine USGS gauging stations.

Accumulated Mean Annual Precipitation. Mean annual precipitation volume for each stream cell was calculated by accumulating the PRISM precipitation data (Water and Climate Center of the Natural Resources Conservation Service, 1998) over the contributing area to the cell. This was calculated concurrently with drainage area, using the algorithms previously described for flow accumulation. The accumulated mean annual precipitation (mm/year) assigned to each reach was the accumulated volume divided by drainage area, both for the downstream-most cell in the reach.

Mean Annual Flow. Mean annual flow (m^3/s) was modeled from drainage area and accumulated mean annual precipitation for each stream cell from the equation of Lorensen et al. (1994) for western Oregon. Each reach was assigned the modeled mean annual flow at the downstream-most cell in the reach. We deviated in applying the Lorensen et al. (1994) equation by replacing the 1993 version of PRISM precipitation data (Daly et al., 1994) with the 1998 version (Water and Climate Center of the Natural Resources Conservation Service, 1998) and by replacing mean annual precipitation estimated only at each flow gauge with the accumulated mean annual precipitation for the area draining to each gauge. To evaluate if these data upgrades proscribed use of the Lorensen et al. (1994) equation, we regressed modeled and measured mean annual flows for reaches on the delineated stream network that contained the nine USGS gauging stations. These gauges had the same period of record as the precipitation data and so were a subset of the gauges used to develop the Lorensen et al. (1994) equation.

Probability of Perennial Flow. We constructed a cumulative distribution function from drainage areas corresponding to the upper limit of field-determined perennial flow for streams in the SNF data. Thus for any given drainage area, we could estimate the probability that a stream is perennial from the proportion of SNF streams with perennial flow. The estimated probability of perennial flow was then assigned from the cumulative distribution function to each reach in the delineated stream network based on drainage area for the reach.

Channel Gradient. Because the DEM elevations were interpolated from contour lines, a point of known elevation occurred wherever a contour crossed an inferred stream channel. Locations of these crossings were estimated by searching for elevations equal to multiples of the contour interval (where hypsography is available, a better method is to directly overlay the DEM with these contours). Modeled channel gradient was calculated for the channel section between consecutive contour-stream crossings by dividing the estimated length of the channel section into the contour interval. With this method, each cell in the delineated stream network was assigned a channel gradient and each reach was assigned the mean value for cells in the reach. Because the estimated channel length associated with each cell varies with flow direction, we used a length-weighted mean.

As an evaluation, we compared modeled channel gradients with channel gradients estimated from 1:24,000-scale USGS topographic maps for a random selection of 20% of the ODF&W reaches ($n = 52$). Channel gradient for a randomly selected point within each reach was calculated for the section of stream between the two contours encompassing the point by dividing the length of the stream section into the contour interval. These map-based gradients were regressed with the modeled gradients for reaches on the delineated stream network that contained the randomly selected points.

We evaluated modeled channel gradients also through regression with field-measured channel gradients for reaches in the ODF&W data. From the field-measured gradients of component habitat units (Moore *et al.*, 2002), we calculated a length-weighted average for each ODF&W reach.

Active-Channel Width. We modeled active-channel width (m) for each stream cell as a power function of modeled mean annual flow (m³/s) (Leopold and Maddock, 1953) using field-measured values for reaches in the ODF&W and EMAP data. Cell-level values were averaged to obtain a reach-level active-channel width. Active-channel width is defined as the estimated distance across the channel at bank-

full flow, which is the maximum streamflow attained every 1.5 years on average (Moore *et al.*, 2002).

Active-Channel Depth. We modeled active-channel depth (m) for each stream cell, following Dunne and Leopold (1978), as a power function of drainage area (km²) using measured values in the data of ODF&W, EMAP, and Castro and Jackson (2001). Cell-level values were averaged to obtain a reach-level active-channel depth. Active-channel depth is defined as the estimated channel depth at bankfull flow (Moore *et al.*, 2002).

Valley-Floor Width. Valley-floor width (m) for each stream cell was modeled as the length of a transect that intersected the valley wall at a distance above the channel elevation equal to five times the active-channel depth. We selected a height of five active-channel depths by visually comparing the 7.5-minute DRG data to valley-floor widths estimated at different multiples of active-channel depth. Each transect was oriented to minimize its length, addressing uncertainties about exact valley orientation and avoiding gross overestimations, particularly at tributary junctions. Therefore, any cell-level valley width that exceeded 2.5 times the median in a centered window of 10 cells was identified as an error and replaced by a linear fit through the remaining values. Cell-level values were averaged to obtain a reach-level valley-floor width.

We evaluated modeled valley-floor widths against widths of the 100-year floodplain on Federal Emergency Management Agency (FEMA) maps (FEMA, 1996, 1998), which are highly accurate but available only for larger rivers. Streams in the delineated network with a drainage area exceeding 180 km² were overlain on a grid of evenly spaced points. For each point that fell on a stream within a 100-year FEMA-mapped floodplain ($n = 124$), the distance was measured twice across the floodplain. The average distance for each point was then regressed with the modeled valley-floor width of the nearest reach to the point.

The modeled valley-floor width was also evaluated in univariate regressions with terrace width and with floodprone width for the subset of ODF&W reaches for which we had these data on smaller wadeable streams. Terrace width (m) is the inter-terrace distance measured between the first high terrace lip on each side of the channel (Moore *et al.*, 2002). Floodprone width (m) is the width of the valley floor inundated during a 50-year return interval flood (Moore *et al.*, 2002).

Valley-Width Index. We calculated the valley-width index as the ratio of the modeled valley-floor

width to the modeled active-channel width for each stream reach. The modeled and field-estimated values of valley-width index were regressed for reaches in the ODF&W data. Valley-width index was estimated in the field for each reach by visually approximating the number of active-channel widths necessary to fill the valley (Moore *et al.*, 2002).

Valley Constraint.   Valley constraint was interpreted relative to field-determined channel-form classes in the ODF&W data (Moore *et al.*, 2002) that best reflected whether a stream reach was confined by adjacent hillslopes. We used ODF&W reaches in the class "constrained by hillslopes" and called these constrained ($n = 91$) and in the two unconstrained classes (anastomosing channel and predominantly single-channel) and called these unconstrained ($n = 33$). None of the ODF&W reaches were classed as "constrained by bedrock" or as "unconstrained-braided." We excluded the one reach in the ODF&W data classed as "constrained by landuse" as well as all reaches classed as either "constrained by terrace" or "alternating terrace and hillslope," because terraces are less permanent features that are not reliably represented in the DEMs.

The difference between the field-determined constrained and unconstrained classes was evaluated with one-way ANOVA on the modeled valley-width index (SAS version 8.2; PROC GLM) for the ODF&W reaches. We analyzed the ranked data because parametric assumptions could not be met.

We identified the group of ODF&W reaches with a modeled valley-width index that was less than or equal to the median for the field-determined constrained class as constrained, or greater than or equal to the median for the field-determined unconstrained class as unconstrained. Agreement between the field-determined classes and identified modeled groups for valley constraint was displayed in a contingency table and evaluated with the correct classification rate and the Cohen's kappa statistic (chance-adjusted correct classification rate) (Lowry, 2006).

Given our findings, we assigned reaches in the modeled stream network a value describing the likelihood of being constrained by adjacent hillslopes. Reaches with a modeled valley-width index that was less than or equal to the median for the field-determined constrained class were assigned a 100% likelihood of being constrained by adjacent hillslopes. Reaches with a modeled valley-width index greater than or equal to the median for the field-determined unconstrained class were assigned a 0% likelihood of being constrained. For reaches with a modeled valley-width index between these medians, a likelihood of being constrained (L_c) between 0 and 100% was

assigned based on a linear equation derived from the medians.

RESULTS AND DISCUSSION

Stream Network Delineation

Figure 4 illustrates that our modeling approach, with channel-initiation thresholds set to 16 m for hillslopes less than 25% (Figure 3a) and to 360 m for steeper slopes (Figure 3b), appeared to delineate streams in the Oregon Coastal Province that were resolved by the digital elevation data. These threshold values can be evaluated or refined if field maps of channel initiation points become available (Lin *et al.*, 2006). The approximately 96,000-km synthetic stream network closely matched the location of 1:24,000-scale USGS hydrography and captured many small streams not represented in that hydrography (Figure 4). Subject to limitations in the DEMs, the modeling approach produced a stream network of consistent density across all land ownerships. The synthetic stream network extended to drainage areas that included the upper-most extent of many, but not all, field-mapped perennial streams. By incorporating dependence on topographic convergence to identify channel initiation points, we were able to extend the stream network to these small drainage areas without "feathering" of channels onto planar hillslopes. This is not possible, as illustrated by Figure 1C, with most available software packages that use standard algorithms lacking sensitivity to local topographic convergence. Because these small streams can provide habitat and can transport food resources, sediment, and wood to larger channels downstream (Gomi *et al.*, 2002; Moore and Richardson, 2003; Bryant *et al.*, 2004), accurate representation is important for assessing stream conditions and for designing riparian protection strategies.

Stream Attributes

Drainage Area.   Values of modeled drainage area were highly correlated and plotted along a 1:1 line with those mapped by ODF&W ($R^2 = 0.99$; df = 265; $p < 0.0001$) and by the USGS ($R^2 = 0.99$; df = 8; $p < 0.0001$). These results indicated that field-surveyed reaches and flow gauges were correctly geo-referenced to the synthetic stream network and that drainage areas were accurately modeled over the ranges in the ODF&W and USGS datasets. This was
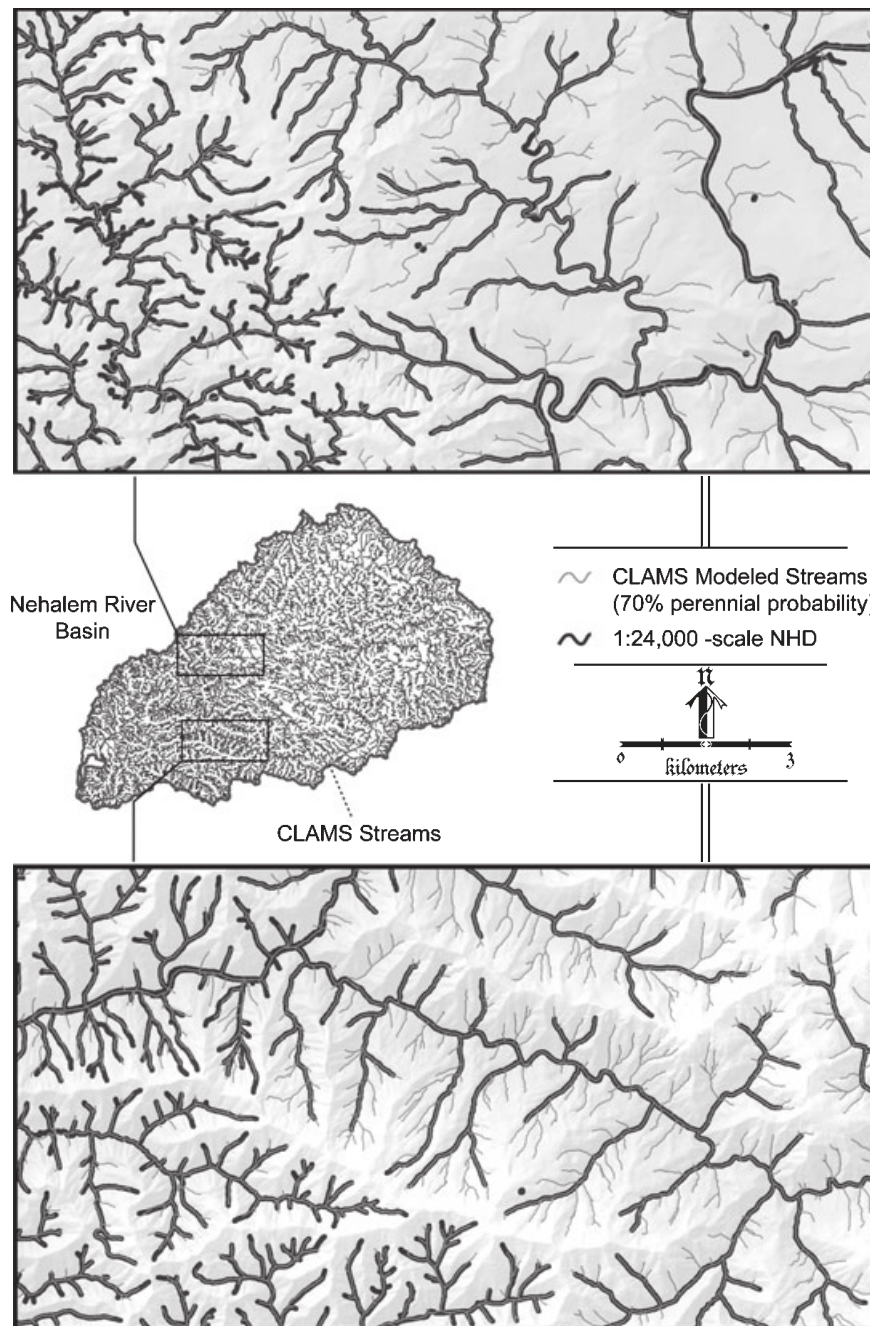
FIGURE 4. Streams Modeled From the 10-m DEMs for an Example Basin in the Oregon
Coastal Province. Outsets show the portion of the delineated stream network identified at a 70%
probability of perennial flow overlaid with hydrography from 1:24,000-scale USGS topographic maps.

important because several other stream attributes were determined as functions of drainage area.

Mean Annual Flow. Modeled mean annual flows were highly correlated with, but somewhat over estimated, field-measured values (Figure 5). As a result, we decided that the Lorensen *et al.* (1994) equation was suitable for modeling mean annual flow from the newly available precipitation estimates. Although a nonlinear equation for mean annual flow, such as that of Lorensen *et al.* (1994), may perform better in regional applications than a linear model, the flow estimate downstream of a confluence will not equal the estimates summed for the two upstream channels. This inconsistency underscored that each modeled value was reasonably accurate but fell within some range of the actual value and influenced our decision not to correct for the slight bias in modeled
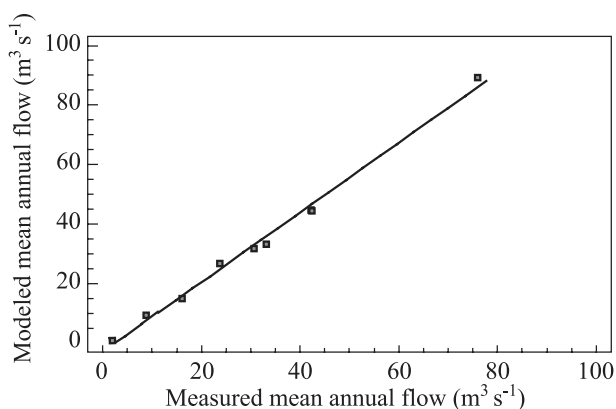
FIGURE 5. Modeled Mean Annual Flow Regressed With Measured Mean Annual (1960-1991) Flow ($R^2 = 0.99$; df = 8; $p < 0.0001$).
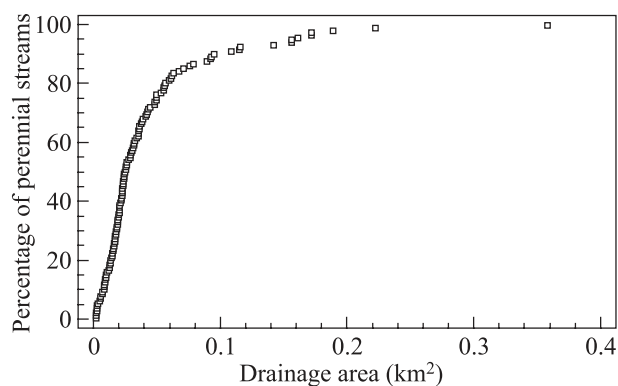

FIGURE 6. Cumulative Distribution Function of Drainage Areas Corresponding to the Upper Limit of Field-Determined Perennial Flow for Streams in the Siuslaw National Forest Dataset.

mean annual flows. If desired later, any overestimation could be easily corrected via the regression relationship between modeled and measured flows.

Estimates of mean annual flow are valuable for evaluating regional riparian policies and for characterizing fish habitat potential. Riparian policies for state and private lands in Oregon differ based on mean annual flow (Young, 2000); riparian management areas are narrower and activities are less restricted along streams with lower flows. Mean annual flow is also a key component in models that assess the potential of streams to provide high-quality habitat for juvenile steelhead and coho salmon (Burnett *et al.*, 2007). Equations are provided in Lorensen *et al.* (1994) to estimate mean annual flow elsewhere in Oregon. Equations for California (e.g., Agrawal *et al.*, 2005) have been incorporated directly into our framework to model flow, which can be done for other areas if mean annual precipitation data are available.

Probability of Perennial Streamflow. Based on the cumulative distribution function in Figure 6, we assumed perennial flow in all reaches with drainage areas greater than 0.36 km^2 but in no reaches with drainage areas less than 0.01 km^2. For intermediate drainage areas, the probability of perennial flow in a reach was estimated from the percentage of SNF streams with perennial flow (Figure 6). For example, at a drainage area of 0.04 km^2, we assign a 70% probability of perennial flow to reaches in the synthetic stream network because 70% of streams in the SNF data had perennial flow (Figure 6). As a point of reference, the delineated network identified at a 70% probability of perennial flow somewhat overestimated the extent of streams on 1:24,000-scale USGS topographic maps (Figure 4). The ability to distinguish perennial streams is beneficial when characterizing current riparian protection or modeling alternatives

because policies may differ between perennial and intermittent stream types (e.g., USDA and USDI, 1994). Until now, these stream types could be differentiated only in the field, and thus, only over small areas for the Oregon Coastal Province.

Although landscape characteristics, such as geology, climate, and land cover, can affect the point of transition to perennial flow, we did not stratify the SNF data by any other dataset and develop multiple cumulative distribution functions. Reasons for the decision are that the resolution of the secondary datasets was generally too coarse to characterize small headwater streams accurately and the spatial extent of the SNF data did not encompass the regional variation in the secondary datasets. To illustrate, when the SNF data were stratified by rock type (Walker and MacLeod, 1991), only three of eight rock types contained more than five observations on the point of perennial flow. Further, the median drainage area at that point did not differ among rock types (Kruskal-Wallis test statistic = 12.52; df = 7; $p = 0.19$). As additional data become available, the cumulative distribution function can be refined, the data can be stratified and new functions developed, or other approaches, such as logistic regression, can be explored for distinguishing perennial streams.

Channel Gradient. Montgomery *et al.* (1998) identified a number of issues that may prevent accurate estimation of channel gradient from DEMs, such as occurrence of pits in the DEM or finer-scale topography that is poorly represented. Our modeling approach alleviated many of these problems, as indicated by the close relationship between modeled channel gradients and those manually determined from 1:24,000-scale USGS topographic maps ($R^2 = 0.94$; df = 51; $p < 0.0001$) (Figure 7a). Channel gradient is a key attribute for characterizing channel

type and response to disturbance (Montgomery and Buffington, 1997), fish habitat (Lunetta *et al.*, 1997; Montgomery *et al.*, 1999; Wyatt, 2003), and streamside areas (Hemstrom *et al.*, 2002). But, both map-derived and DEM-derived estimates may differ from gradients measured in the field, which are the values with potential to affect stream ecosystems.

Field-measured and modeled channel gradients were highly correlated for stream reaches in the ODF&W data (Figure 7b). However, the resulting regression relationship suggested that field-measured gradients were overestimated at modeled gradients exceeding 1.08%. Isaak *et al.* (1999) obtained similar results for streams in Wyoming. A partial explanation for such overestimations is that, for a given stream section, measured length increases as the measurement resolution becomes finer (Mueller, 1979; Mark, 1983). Therefore, field-measured stream lengths are expected to be greater than coarser-resolution DEM-estimated lengths, and differences between the two should increase as the terrain becomes more complex. Likewise, gradient, which is

change in elevation divided by reach length, is expected to differ more between field-derived and DEM-derived estimates in more complex, higher gradient terrain. To better reflect stream conditions and distributions of salmonids, we calibrated modeled channel gradients using the regression relationship with measured field gradients (Figure 7). We chose not to calibrate modeled gradients greater than 20%, because few ODF&W reaches had field gradients exceeding this. Both calibrated and un-calibrated gradients were included in model output files.

As illustrated in Figure 8, modeled channel gradient can be used to map the likely extent of salmonid distribution. In this example, similar to Burnett *et al.* (2007), we assumed use by coho salmon in areas downstream of reaches with modeled gradients exceeding 7%. The gradient calibration improved the ability to approximate the coho-salmon-bearing stream network as mapped by ODF&W (2003) (Figure 8). Analogously, the fish-bearing portion of the stream network could be mapped by assuming use in any reach downstream of modeled gradients exceeding 20%, consistent with guidance provided by the Oregon Department of Forestry (1997). Because riparian policies for both public and private lands are typically more restrictive along fish-bearing streams (USDA and USDI, 1994; Young, 2000), distinguishing between potentially fish-bearing and nonfish-bearing portions of stream networks allows decision makers to evaluate differences between riparian policies over broad spatial extents.

Active-Channel Width. The empirical relationship we derived to estimate active-channel widths (Figure 9) is consistent with those for other areas with relatively high precipitation (e.g., Leopold *et al.*, 1964; McKerchar *et al.*, 1998). The relationship predicts that active-channel width increases consistently in the downstream direction. Although generally true, local sources of variability, such as bedrock nick points, can affect habitat potential but are not reflected in this broad-scale relationship. Active-channel width indicates flows critical for shaping and maintaining channel morphology over time and is commonly applied to describe stream size and to evaluate the potential for a stream to interact with its floodplain.

Active-Channel Depth. The empirical relationship to estimate active-channel depths (Figure 10) approximated that of Ghizzoni *et al.* (2006) and fit the data better than the analogous relationship based on flow. Active-channel depth reflects flows critical for shaping and maintaining channel morphology and was needed in our approach for calculating valley-floor width.
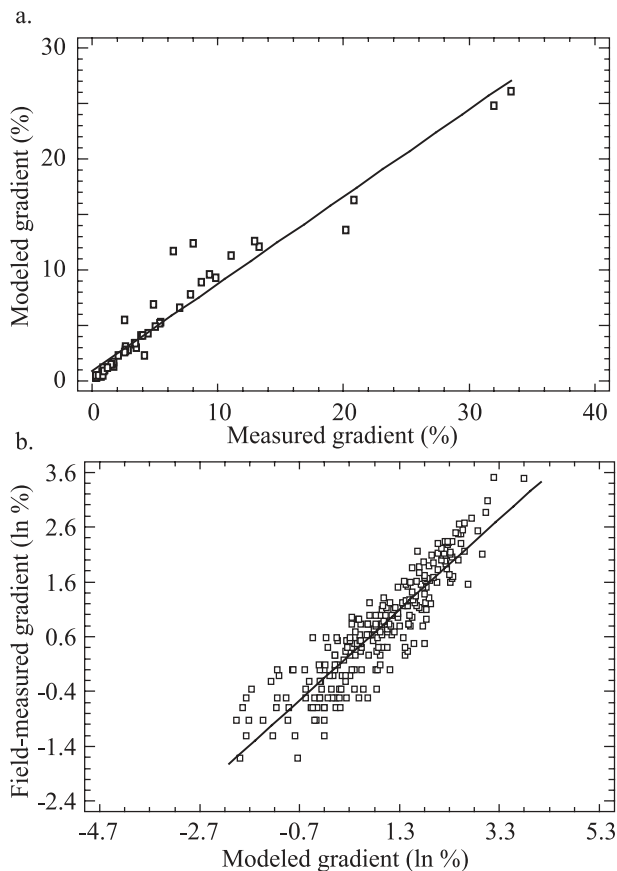

FIGURE 7. Modeled Channel Gradients (S_m) Regressed With (a) Map-Measured Gradients and (b) Field-Measured Gradients (S_f) $\ln(S_f) = 0.02 + 0.83 \times \ln(S_m)$ ($R^2 = 0.82$; df = 251; $p < 0.0001$).
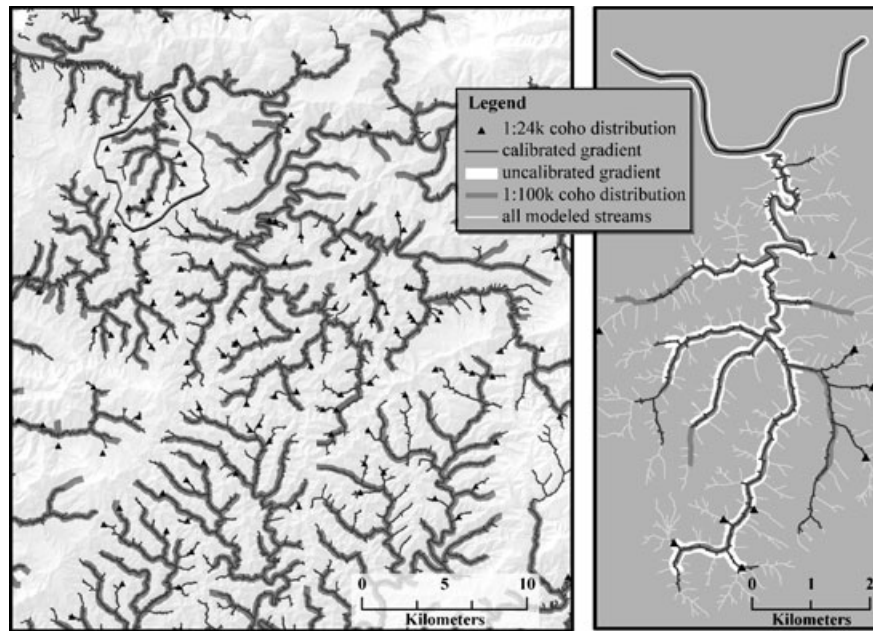
FIGURE 8. Map Comparing Distributions of Coho Salmon Based on Modeled Channel Gradient and as Estimated by the ODF&W. The portion of the modeled stream network downstream of reaches with calibrated gradients exceeding 7% was identified to approximate the distribution of coho salmon. The portion downstream of reaches with uncalibrated gradients exceeding 7% is shown for comparison. The distribution of coho salmon as estimated by ODF&W is mapped continuously at the 1:100,000 scale and as only end points at the 1:24,000 scale.
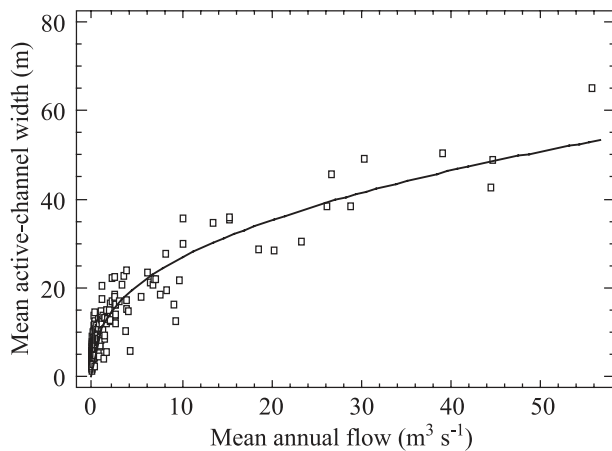

FIGURE 9. Relationship Between Field-Measured Mean Active-Channel Width (W_a) and Modeled Mean Annual Flow (Q) ($W_a = 10.70 \times Q^{0.40}$) ($R^2 = 0.89$; df = 271; $p < 0.0001$).
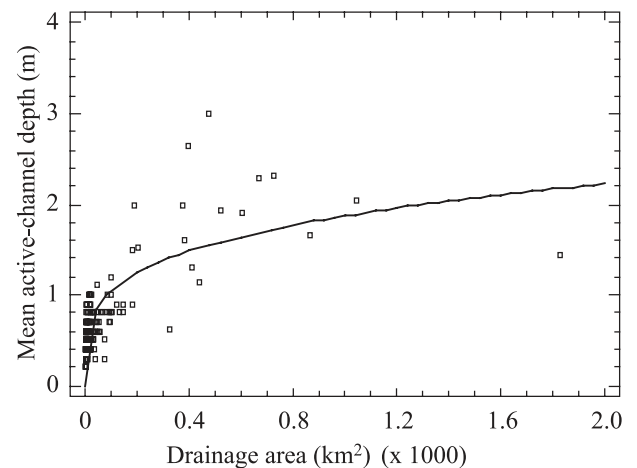

FIGURE 10. Relationship Between Field-Measured Mean Active-Channel Depth (H_a) and Modeled Drainage Area (D) ($H_a = 0.328 \times D^{0.252}$) ($R^2 = 0.64$; df = 273; $p < 0.0001$).

Valley-Floor Width. Limited availability of appropriate measures hampered evaluation of valley-floor widths across all stream sizes. Modeled valley-floor widths for larger streams were reasonably correlated with width measurements from points along 100-year floodplains mapped by FEMA (Figure 11). Our reach-scale estimates averaged out variation represented by point estimates of valley width from the FEMA maps. Modeled valley-floor width was weakly

related to the floodprone width ($R^2 = 0.15$; df = 239; $p < 0.0001$) and to the terrace width ($R^2 = 0.22$; df = 239; $p < 0.0001$) in the ODF&W data. These widths were narrower than the modeled valley-floor width for almost every reach, which was expected given the field measures were not defined as the 100-year floodplain. Consequently, we considered neither of the ODF&W measures appropriate to evaluate valley-floor widths for smaller streams not mapped by FEMA.
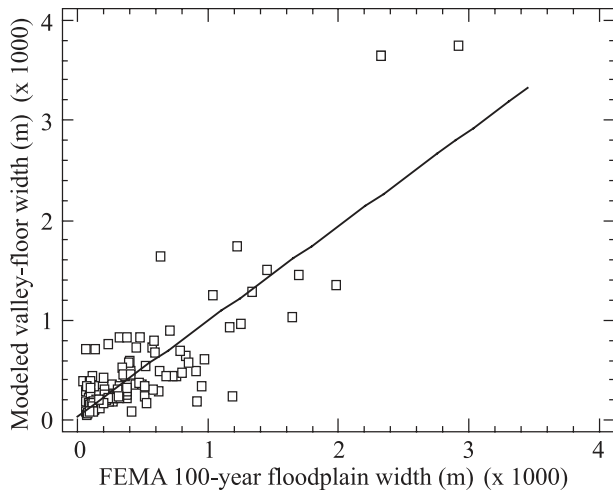
FIGURE 11. Modeled Valley-Floor Width Regressed
Against 100-Year Floodplain Width Mapped by FEMA
for Larger Streams ($R^2 = 0.70$; df = 118; $p < 0.0001$).

Dimensionless rating curves for the Cascade Range in Washington, indicate a 100-year recurrence flow at 2.2 times the active-channel depth (Dunne and Leopold, 1978), rather than at five times the active-channel depth for which we modeled valley-floor widths. Our choice in part reflected the ability to resolve valley topography with available DEM data. Had we chosen a smaller value, modeled valley-floor widths would have been narrower and underestimated 100-year floodplain widths on FEMA maps but might have been more highly correlated with the ODF&W width estimates.

Valley floors have been identified in other modeling efforts (Hemstrom et al., 2002; Gallant and Dowling, 2003; Noman et al., 2003), however this is the only study of which we are aware that explicitly links measurements of valley-floor width to a synthetic stream network. Variations in valley width influence the suite of processes that move sediment, water, and wood into and through channels and thus affect characteristics of stream habitat, floodplains, and riparian areas of concern to managers. Wide valleys can store wood and sediment in which self-formed alluvial channels and associated habitats can develop (McDowell, 2001), but channels in such valleys can be prone to the negative effects of land management that increase sediment delivery rates or limit interaction between the stream and its floodplain (e.g., IMST, 1999). Narrow valleys offer fewer storage opportunities and tend to transport sediment. Longitudinal variations in valley width create local zones of hyporheic inflow and outflow (Edwards, 1998; Malard et al., 2002) that affect where salmon and trout spawn (Baxter and Hauer, 2000; Geist et al., 2002). Thus,

comprehensive information on valley width that is linked to a digital stream network can inform strategic planning and help focus conservation and restoration activities.

Valley-Width Index. Modeled and field-estimated values of valley-width index were weakly related ($R^2 = 0.20$; df = 264; $p < 0.0001$). This may have several explanations, including that the field value is not based on an independent estimate of the 100-year floodplain width. Alternatively, valley-floor widths, and thus valley-width indices, modeled at the 10-m DEM resolution may be less accurate for small than large streams. However, field data were not available to quantitatively assess this.

Stream reaches with higher values of the valley-width index (>2.5), as determined in the field, are generally thought to have greater potential to interact with their floodplain and greater sensitivity to land-management effects. These unconstrained areas are more likely to have deeper pools, more wood, enlarged hyporheic zones, and complex channel patterns (Gregory et al., 1991; Montgomery and Buffington, 1997; Edwards, 1998; Buffington et al., 2002) that can influence the species and abundances of fish found there (Hicks, 1990; Nickelson, 1998; Baxter and Hauer, 2000; Burnett, 2001). Unconstrained valleys tend to be depositional zones and so may be especially susceptible to land-management effects (Frissell, 1992; Montgomery and Buffington, 1997; Montgomery et al., 1999). Due to the importance of unconstrained areas, we were hesitant to directly interpret our modeled outputs relative to the valley-width index of ODF&W and decided to classify reaches based on the potential for constraint by adjacent hillslopes.

Valley Constraint. Medians of the modeled valley-width index differed for the field-determined constrained class and unconstrained class (Figure 12). Based on the medians, we identified ODF&W reaches as constrained if the modeled valley-width index was ≤5.06 and as unconstrained if the modeled valley-width index was ≥8.87. Groups identified from the modeled valley-width index agreed reasonably well with the field-determined classes of valley constraint (Table 2). We were most concerned about reaches that were truly unconstrained being incorrectly assigned to the constrained group; the 8% commission error rate indicates that this was relatively unlikely.

According to these findings, we assigned each reach in the modeled stream network a likelihood of being constrained by adjacent hillslopes. A 100% likelihood of being constrained was assigned to reaches with a modeled valley-width index less than
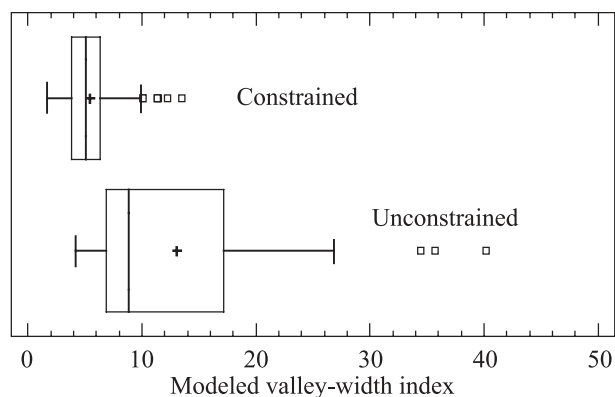
FIGURE 12. Modeled Values of the Valley-Width Index for Field-Determined Constrained and Unconstrained Classes. Boxes designate the 25th and 75th percentiles, the solid line indicates the median, and the plus sign the mean, whiskers denote the nearest data point within 1.5 times the interquartile range, and outliers are shown by disconnected points. The modeled valley-width index differed between the field-determined constrained (median = 5.06) and unconstrained (median = 8.87) classes (Kruskal-Wallis test: $\chi^2 = 43.89$; df = 1; $p < 0.0001$).

likelihood of being constrained to an inordinate number of these streams. It is possible that the valley-floor width was overestimated for small, headwater streams either because it was modeled at a distance too far above the channel or the resolution of the DEM was too coarse. Even a slight overestimation can inflate the valley-width index given that modeled active-channel widths were less than 1 m for many of these small streams, considerably less than the 10-m width of a DEM cell. Another possible explanation is scale-related in that the valley-width index was developed for larger, perennially flowing, fish-bearing streams to differentiate those with well-developed floodplains and so may not be relevant for smaller, intermittent, nonfish-bearing streams. In light of these considerations, the valley-width index and associated valley constraint is reasonably interpreted only for larger streams in the fish-bearing portion of the modeled network (i.e., downstream of gradients in excess of 20%).

or equal to the median for the field-determined constrained class. A 0% likelihood of being constrained was assigned to reaches with a modeled valley-width index greater than or equal to the median for the field-determined unconstrained class. For reaches with a modeled valley-width index between these two median values, a likelihood between 0 and 100% of being constrained (L_c) was assigned as $L_c = 233 - 26\ v$, where v is the valley-width index. Thus, for example, reaches with a modeled valley-width index of 8.0 were assigned a 25% likelihood of being constrained while reaches with a modeled valley-width index of 6.0 were assigned a 77% likelihood.

When we examined the assigned likelihood of being constrained relative to the 7.5-minute-DRG data, results were generally as expected except for small, headwater streams. Such streams are often in relatively steep, narrow valleys (Montgomery *et al.*, 1998), and so our approach appeared to assign a low

USES AND LIMITATIONS

Our modeling effort was motivated by the needs of decision makers for information on the location and characteristics of streams across entire landscapes. Spatially, continuous fine-grained information on streams is limited to relatively small areas due to the high costs of acquiring, storing, and processing field and remote sensing data (e.g., LiDAR). Regionally extensive digital datasets (e.g., USGS 10-m DEMs and PRISM climate data) do exist, and although stream networks and attributes cannot be measured directly from these, they may be modeled. Consequently, we developed, adapted, and integrated a suite of models that use such digital datasets to delineate a high-resolution synthetic stream network and stream attributes necessary for inferring habitat potential and disturbance susceptibility across a large area. We capitalized on available field data to

TABLE 2. Agreement Between Field-Determined Classes of ODF&W and Groups Identified Based on the Modeled Valley-Width Index.

| | | Identified Group | | | Percent |
		Constrained	Unconstrained	Total	Correct
Field-Determined	Constrained	46	11	57	81
Class	Unconstrained	4	17	21	81
	Total	50	28	78	81
	Percent Correct	92	61		

Notes: With the method in Lowry (2006), the chance-adjusted correct classification rate (Cohen's kappa statistic) is 71%, expressed as a percentage of the maximum possible correct classification ($0.56/0.79 \times 100$) based on the observed marginal frequencies of 50 (constrained reaches) and 21 (unconstrained reaches).

estimate and interpret numerous stream attributes by establishing empirical relationships with features derivable from the digital datasets. Taking advantage of strengths in both digital and field data, our modeling approach can contribute to broad-scale management, regulatory, and research efforts for streams in the Oregon Coastal Province and elsewhere.

The modeled stream network and attributes have been used to consider management of riparian forests. For example, potential effects of riparian policies on forest cover were projected across the Oregon Coastal Province for riparian areas determined using our stream network (Bettinger *et al.*, 2005; Spies *et al.*, 2007). Additionally, Burnett and Miller (2007) used reach-specific estimates of channel gradient and valley width, coupled with empirical models of landsliding, to identify headwater channels through which wood and sediment were likely to be transported in debris flows to larger fish-bearing streams. Information on which headwater channels may be future sources of wood recruitment can aid in developing regional riparian management policies that are efficient and effective.

Outputs of our modeling approach have been widely used to characterize the potential of streams to provide high-quality habitat for salmonids. The stream network and attributes describing habitat potential (gradient, mean annual flow, and valley constraint) were used across the entire Oregon Coastal Province to assess the quality and quantity of coho salmon habitat made available by past culvert repair and replacements (Dent *et al.*, 2005); to locate areas of high habitat potential for coho salmon and steelhead relative to land ownership, use, and cover (Burnett *et al.*, 2007); and as inputs to estimate the maximum production potential of coho salmon smolts for consideration in ESA recovery planning (Lawson *et al.*, 2005). Agrawal *et al.* (2005) adapted the approach to model a stream network and habitat potential for coho salmon, winter steelhead, and fall-run Chinook salmon throughout southwestern Oregon and northern California by recalibrating some of the regression relationships we presented and excluding areas that were naturally too warm for salmon. The stream modeling approach has also been applied to evaluate the quantity of habitat blocked by anthropogenic barriers in the Willamette and Lower Columbia River basins (Sheer and Steel, 2006) and by dams in the California Central Valley (Lindley *et al.*, 2006).

Although modeled outputs can be directed toward a variety of purposes that require a high-resolution stream network and spatially continuous estimates of stream attributes, the level of confidence to place in these outputs depends on many factors. As our evaluations indicated, some stream attributes (e.g., gradi-

ent) were more likely than others (e.g., valley width) to accurately represent field conditions or be directly comparable to available field data. Variation in the accuracy, precision, and resolution of GIS data can also add to uncertainty in modeled outputs. For example, variations in density (km/km^2) of modeled streams arose in part from variations across the Coastal Province in the degree to which contour crenulations are represented in the 1:24,000-scale USGS topographic maps and, consequently, in the DEMs derived from those maps. Field measurements, generally considered accurate, were lacking for some stream attributes in some areas (e.g., probability of perennial flow in basalt rock types). Therefore, empirical relationships were extrapolated to areas without field-measured values, increasing uncertainty in those estimates. The number of field measurements were insufficient for some stream types (e.g., reaches in larger rivers, very small streams, and unconstrained reaches) to allow model building and testing on different datasets and so derived empirical relationships could not be independently evaluated for all stream attributes.

In general, we are most confident in the reach-scale outputs for mid-order and larger streams, because these were best represented in the available field data. Even so, outputs should be cautiously applied for reach-specific analyses and are most reliable when summarized and interpreted over watersheds or larger spatial extents. Over larger areas natural variability and other sources of uncertainty are more likely to be averaged out. Given the reliance on field measurements, the modeling approach may have limited applicability in regions lacking stream attribute data that are available for the Oregon Coastal Province. However, our results can inform data collection strategies in such areas to include geo-referenced field measurements needed to model stream attributes.

CONCLUSIONS

Combining field measurements with digital data to delineate a synthetic stream network and estimate stream attributes is a practical alternative to either fine-grained field or remote sensing methods (e.g., LiDAR) for regional mapping of aquatic resources. With a combined approach, we delineated a stream network for the Oregon Coastal Province that matched the location of streams on USGS 1:24,000-scale topographic maps, consistently represented many small streams that were not mapped in the USGS hydrography, and minimized artifact

streams. Incorporating field data increases confidence in the modeled values of stream attributes and allows attributes to be modeled that would not be possible solely from the digital data. Broad-scale assessment of streams for management, regulation, and research is facilitated by having a wide variety of attributes linked to a high-resolution stream network. The accuracy and thus the utility of any mapped stream outputs are limited by the quality of the digital and field data used in their production. Outputs for the Oregon Coastal Province can be improved if data of higher quality or from underrepresented areas become available. Because our stream modeling approach is flexible, outputs for other regions can be modeled if the necessary digital and field data exist or can be obtained.

LITERATURE CITED

Agrawal, A., R.S. Schick, E.P. Bjorkstedt, R.G. Szerlong, M.N. Goslin, B.C. Spence, T.H. Williams, and K.M. Burnett, 2005. Predicting the Potential for Historical Coho, Chinook and Steelhead Habitat in Northern California, NOAA Technical Memorandum NOAA-TM-NMFS-SWFSC-379, 25 pp.

Baxter, C.V. and F.R. Hauer, 2000. Geomorphology, Hyporheic Exchange, and Selection of Spawning Habitat by Bull Trout (*Salvelinus Confluentus*). Canadian Journal of Fisheries and Aquatic Sciences 57:1470-1481.

Benda, L.E., K. Andras, D.J. Miller, and P. Bigelow, 2004. Confluence Effects in Rivers: Interactions of Basin Scale, Network Geometry, and Disturbance Regimes. Water Resources Research 40:1-15, W05402. doi: 10.1029/2003SR002583.

Bettinger, P., M. Lennette, K.N. Johnson, and T.A. Spies, 2005. A Hierarchical Spatial Framework for Forest Landscape Planning. Ecological Modelling 182:25-48.

Bryant, M.D., N.D. Zymonas, and B.E. Wright, 2004. Salmonids on the Fringe: Abundance, Species Composition, and Habitat Use of Salmonids in High-Gradient Headwater Streams, Southeast Alaska. Transactions of the American Fisheries Society 133(6):1529-1538.

Buffington, J.M., T.E. Lisle, R.D. Woodsmith, and S. Hilton, 2002. Controls on the Size and Occurrence of Pools in Coarse-Grained Forest Rivers. River Research and Applications 18(6):507-531.

Burnett, K.M., 2001. Relationships Among Juvenile Anadromous Salmonids, Their Freshwater Habitat, and Landscape Characteristics Over Multiple Years and Spatial Scales in Elk River, Oregon. Ph.D. Dissertation, Oregon State University, Corvallis, Oregon.

Burnett, K.M. and D.J. Miller, 2007. Streamside Policies for Headwater Channels: An Example Considering Debris Flows in the Oregon Coastal Province. Forest Science 53:239-253.

Burnett, K.M., G.H. Reeves, S.E. Clarke, and K.R. Christiansen, 2006. Comparing Riparian and Catchment Influences on Stream Habitat in a Forested, Montane Landscape. *In:* Landscape Influences on Stream Habitats and Biological Assemblages, Robert M. Hughes, Lizhu Wang, and Paul Seelbach (Editors). American Fisheries Society, Bethesda, Maryland, pp. 175-197.

Burnett, K.M., G.H. Reeves, D.J. Miller, S. Clarke, K. Vance-Borland, and K. Christiansen, 2007. Distribution of Salmon-Habitat Potential Relative to Landscape Characteristics and Implications for Conservation. Ecological Applications 17(1):66-80.

Castro, J.M. and P.L. Jackson, 2001. Bankfull Discharge Recurrence Intervals and Regional Hydraulic Geometry Relationships: Patterns in the Pacific Northwest, USA. Journal of the American Water Resources Association 37(5):1249-1262.

Clarke, S.E. and K.M. Burnett, 2003. Comparison of Digital Elevation Models for Aquatic Data Development. Photogrammetric Engineering and Remote Sensing 69(12):1367-1375.

Daly, C., R.P. Neilson, and D.L. Phillips, 1994. A Statistical Topographic Model for Mapping Climatological Precipitation Over Mountainous Terrain. Journal of Applied Meteorology 33:140-158.

Davies, J.R., K.M. Lagueux, B. Sanderson, and T.J. Beechie, 2007. Modeling Stream Channel Characteristics From Drainage-Enforced DEMs in Puget Sound, Washington, USA. Journal of the American Water Resources Association 43:414-426.

Dent, L., A. Herstrom, and E. Gilbert, 2005. A Spatial Evaluation of Habitat Access Conditions and Oregon Plan Fish Passage Improvement Projects in the Coastal Coho ESU, Oregon Plan Technical Report 2, 24 pp. http://nrimp.dfw.state.or.us/OregonPlan/, *accessed* January 2006.

Dietrich, W.E., C.J. Wilson, D.R. Montgomery, J. McKean, and R. Bauer, 1992. Erosion Thresholds and Land Surface Morphology. Geology 20:675-679.

Dunham, J.B., B.S. Cade, and J.W. Terrell, 2002. Influences of Spatial and Temporal Variation on Fish-Habitat Relationships Defined by Regression Quantiles. Transactions of the American Fisheries Society 131:86-98.

Dunne, T. and L.B. Leopold, 1978. Water in Environmental Planning. W.H. Freeman and Company, San Francisco, California.

DWAF (Department of Water Affairs and Forestry), 2006. South Africa 1:500,000 Rivers. http://www.dwaf.gov.za/iwqs/gis_data/river/rivs500k.html, *accessed* April 2006).

Edwards, R.T., 1998. The Hyporheic Zone. In: River Ecology and Management: Lessons From the Pacific Coastal Ecoregion, R.J. Naiman and R.E. Bilby (Editors). Springer-Verlag, New York, New York, pp. 399-429.

ESA (Endangered Species Act), 1973. Endangered Species Act of 1977. Public Law 93-205.

ESRI (Environmental Systems Research Institute), 1998. ESRI Shapefile Technical Description. Environmental Systems Research Institute, Redlands, California. http://www.esri.com/library/whitepapers/pdfs/shapefile.pdf, *accessed* June 2006.

FEMA (Federal Emergency Management Agency), 1996. Publication Dates of All Maps Used Except for the Coquille River. Flood Insurance Maps. http://www.fema.gov, *accessed* May 2006.

FEMA (Federal Emergency Management Agency), 1998. Map for the Coquille River. Flood Insurance Maps. http://www.fema.gov, *accessed* May 2006.

FEMAT (Forest Ecosystem Management Assessment Team), 1993. Forest Ecosystem Management: An Ecological, Economic, and Social Assessment. U.S. Department of Agriculture and U.S. Department of the Interior, Portland, Oregon.

Flitcroft, R.L., K.K. Jones, K.E.M. Reis, and B.A. Thom, 2002. Year 2000 Stream Habitat Conditions in Western Oregon. Monitoring Program Report OPSW-ODFW-2001-05, Oregon Department of Fish and Wildlife, Portland, Oregon, 41 pp.

Frissell, C.A., 1992. Cumulative Effects of Land-Use on Salmon Habitat in Southwest Oregon Coastal Streams. Ph.D. Dissertation, Oregon State University, Corvallis, Oregon.

Gallant, J.C. and T.I. Dowling, 2003. A Multiresolution Index of Valley Bottom Flatness. Water Resources Research 39(12):4-1-4-13.

Ganio, L.M., C.E. Torgersen, and R.E. Gresswell, 2005. A Geostatistical Approach for Describing Spatial Pattern in Stream Networks. Frontiers in Ecology and the Environment 3(3):138-144.

Garbrecht, J. and L.W. Martz, 1997. The Assignment of Drainage Direction Over Flat Surfaces in Raster Digital Elevation Models. Journal of Hydrology 193:204-213.

Geist, D.R., T.P. Hanrahan, E.V. Arntzen, G.A. McMichael, C.J. Murray, and Y. Chien, 2002. Physicochemical Characteristics of the Hyporheic Zone Affect Redd Site Selection by Chum Salmon and Fall Chinook Salmon in the Columbia River. North American Journal of Fisheries Management 22:1077-1085.

Geoscience Australia, 2003. GEODATA TOPO 250K Series 2: Product User Guide. National Mapping Division, Geoscience Australia, Canberra, Australian Capital Territory.

Ghizzoni, T., M. Lomazzi, G. Rothl, and R. Rudari, 2006. Regional Scale Analysis of the Altimetric Stream Network Evolution. Advances in Geosciences 7:79-83.

Gomi, T., R.C. Sidle, and J.S. Richardson, 2002. Understanding Processes and Downstream Linkages of Headwater Systems. BioScience 52:905-916.

Gregory, S.V., F.J. Swanson, W.A. McKee, and K.W. Cummins, 1991. An Ecosystem Perspective of Riparian Zones. BioScience 41(8):540-551.

Hankin, D.G. and G.H. Reeves, 1988. Estimating Total Fish Abundance and Total Habitat Area in Small Streams Based on Visual Estimation Methods. Canadian Journal of Fisheries and Aquatic Sciences 45:834-844.

Hansen, W.F., 2001. Identifying Stream Types and Management Implications. Forest Ecology and Management 143:39-46.

Hemstrom, M.A., T. Smith, D. Evans, C. Clifton, E. Crowe, and M. Aitken, 2002. Midscale Analysis of Streamside Characteristics in the Upper Grande Ronde Subbasin, Northeastern Oregon. USDA Forest Service Research Note PNW-RN-534, Pacific Northwest Research Station, Portland, Oregon, 16 pp.

Herlihy, A.T., D.P. Larsen, S.G. Paulsen, N.S. Urquhart, and B.J. Rosenbaum, 2000. Designing a Spatially Balanced, Randomized Site Selection Process for Regional Stream Surveys: The EMAP Mid-Atlantic Pilot Study. Environmental Monitoring Assessment 63:95-113.

Hicks, B.J., 1990. The Influence of Geology and Timber Harvest on Channel Morphology and Salmonid Populations in Oregon Coast Range Streams. Ph.D. Dissertation, Oregon State University, Corvallis, Oregon.

IMST (Independent Multidisciplinary Science Team), 1999. Recovery of Wild Salmonids in Western Oregon Forests: Oregon Forest Practices Act Rules and the Measures in the Oregon Plan for Salmon and Watersheds. Technical Report 1991-1 to the Oregon Plan for Salmon and Watersheds. Governor's Natural Resources Office, Salem, Oregon.

Isaak, D.J., W.A. Hubert, and K.L. Krueger, 1999. Accuracy and Precision of Stream Reach Water Surface Slopes Estimated in the Field and From Maps. North American Journal of Fisheries Management 19:141-148.

Jenson, S.K. and J.O. Domingue, 1988. Extracting Topographic Structure From Digital Elevation Data for Geographic Information System Analysis. Photogrammetric Engineering and Remote Sensing 54:1593-1600.

Lawson, P.W., E. Bjorkstedt, M. Chilcote, C. Huntington, J. Mills, K. Moore, T.E. Nickelson, G.H. Reeves, H.A. Stout, and T.C. Wainwright, 2005. Identification of Historical Populations of Coho Salmon (*Oncorhynchus Kisutch*) in the Oregon Coast Evolutionarily Significant Unit. Review Draft, Oregon Northern California Coast Technical Recovery Team, NOAA/NMFS/NWFSC, 129 pp.

Leopold, L.B. and T. Maddock, Jr, 1953. The Hydraulic Geometry of Stream Channels and Some Physiographic Implications. U.S. Geological Survey Professional Paper 252, Washington, D.C., 57 pp.

Leopold, L.B., M.G. Wolman, and J.P. Miller, 1964. Fluvial Processes in Geomorphology. Dover Publications, Inc., New York, New York.

Lin, W.-T., W.-C. Chou, C.-Y. Lin, P.-H. Huang, and J.-S. Tsai, 2006. Automated Suitable Drainage Network Extraction From Digital Elevation Models in Taiwan's Upstream Watersheds. Hydrological Processes 20:289-306.

Lindley, S.T., R.S. Schick, A. Agrawal, M. Goslin, T.E. Pearson, E. Mora, J.J. Anderson, B. May, S. Greene, C. Hanson, A. Low, D. McEwan, R.B. MacFarlane, C. Swanson, and J.G. Williams, 2006. Historical Population Structure of Central Valley Steelhead and Its Alteration by Dams. San Francisco Estuary and Watershed Science 4(1):1-19, Article 3. http://repositories.cdlib.org/jmie/sfews/vol4/iss1/art3, *accessed* February 5, 2008.

Lorensen, T., C. Andrus, and J. Runyon, 1994. Oregon Forest Practices Act Water Protection Rules: Scientific and Policy Considerations. Forest Practices Policy Unit, Oregon Department of Forestry, Salem, Oregon.

Lowry, R., 2006. Kappa as a Measure of Concordance in Categorical Sorting. http://www.faculty.vassar.edu/lowry/kappa.html with explanation at http://faculty.vassar.edu/lowry/kappaexp.html, *accessed* September 2007.

Lunetta, R.S., B.L. Cosentino, D.R. Montgomery, E.M. Beamer, and T.J. Beechie, 1997. GIS-Based Evaluation of Salmon Habitat for Prioritizing Restoration Opportunities in the Pacific Northwest. Photogrammetric Engineering & Remote Sensing 63:1219-1229.

Malard, F., K. Tockner, M.J. Dole-Olivier, and J.V. Ward, 2002. A Landscape Perspective of Surface-Subsurface Hydrological Exchanges in River Corridors. Freshwater Biology 47:621-640.

Mark, D.M., 1983. Relations Between Field-Surveyed Channel Networks and Map-Based Geomorphometric Measures, Inez, Kentucky. Annals of the Association of American Geographers 73:358-372.

McDowell, P.F., 2001. Spatial Variations in Channel Morphology at Segment and Reach Scales, Middle Fork John Day River, Northeastern Oregon. *In:* Geomorphic Processes and Riverine Habitat, Vol. 4, J.M. Dorava, D.R. Montgomery, B.B. Palcsak, and F.A. Fitzpatrick (Editors). American Geophysical Union, Washington, D.C., pp. 159-172.

McKerchar, A.I., R.B. Ibbitt, S.L.R. Brown, and M.J. Duncan, 1998. Data for Ashley River to Test Channel Network and River Basin Heterogeneity Concepts. Water Resources Research 34(1):139-142.

Montgomery, D.R., E.M. Beamer, G.R. Pess, and T.P. Quinn, 1999. Channel Type and Salmonid Spawning Distribution and Abundance. Canadian Journal of Fisheries and Aquatic Sciences 56:377-387.

Montgomery, D.R. and J.M. Buffington, 1997. Channel-Reach Morphology in Mountain Drainage Basins. Geological Society of America Bulletin 109(5):596-611.

Montgomery, D.R., W.E. Dietrich, and K. Sullivan, 1998. The Role of GIS in Watershed Analysis. *In:* Landform Monitoring, Modeling and Analysis, S.N. Land, K.S. Richards, and J.H. Chandler (Editors). John Wiley and Sons, Hoboken, New Jersey, pp. 241-261.

Montgomery, D.R. and E. Foufoula-Georgiou, 1993. Channel Network Source Representation Using Digital Elevation Models. Water Resources Research 29:3925-3934.

Moore, K., K.K. Jones, and J. Dambacher, 2002. Methods for Stream Habitat Surveys Aquatic Inventories Project. Natural Production Program, Oregon Department of Fish and Wildlife, Corvallis, Oregon. http://oregonstate.edu/Dept/ODFW/freshwater/inventory/pdffiles/habmethod.pdf, *accessed* June 2006.

Moore, D. and J.S. Richardson, 2003. Progress Towards Understanding the Structure, Function, and Ecological Significance of Small Stream Channels and Their Riparian Zones. Canadian Journal of Forest Research 33:1349-1351.

Mueller, J.E., 1979. Problems in the Definition of Measurement of Stream Length. Professional Geographer 31:306-311.

Nickelson, T.E., 1998. A Habitat-Based Assessment of Coho Salmon Production Potential and Spawner Escapement Needs for Oregon Coastal Streams. Information Reports 98-4, Oregon Department of Fish and Wildlife, Portland, Oregon.

Noman, N.S., E.J. Nelson, and A.K. Zundel, 2003. Improved Process for Floodplain Delineation From Digital Terrain Models. Journal of Water Resources Planning and Management 129(5):427-436.

O'Callaghan, J.F. and D.M. Mark, 1984. The Extraction of Drainage Networks From Digital Elevation Data. Computer Vision, Graphics, and Image Processing 28:323-344.

ODF&W (Oregon Department of Fish and Wildlife), 2003. Natural Resources Information Management Program's Fish Distribution Maps. http://rainbow.dfw.state.or.us/nrimp/information/fishdistmaps.htm, *accessed* June 2006.

ODF&W (Oregon Department of Fish and Wildlife), 2007. Sampling Design and Statistical Analysis Methods for the Integrated Biological and Physical Monitoring of Oregon Streams. Report Number: OPSW-ODFW-2002-07. http://nrimp.dfw.state.or.us/crl/default.aspx?p=386, *accessed* September 2007.

Oregon Department of Forestry, 1997. Forest Practice Rule Guidance for OAR-629-635 Water Protection Rules: Purpose, Goals, Classification, and Riparian Management Areas. http://egov.oregon.gov/ODF/Private_Forests/docs/fp/guidance/OARDiv635.pdf, *accessed* June 2006.

Pess, G.R., R. Montgomery, E.A. Steel, R.E. Bilby, B.E. Feist, and H.M. Greenberg, 2002. Landscape Characteristics, Land Use, and Coho Salmon *(Oncorhynchus Kisutch)* Abundance, Snohomish River, Washington, U.S.A. Canadian Journal of Fisheries and Aquatic Sciences 59:613-623.

Reeves, G.H., D.B. Hohler, D.P. Larsen, D.E. Busch, K. Kratz, K. Reynolds, K.F. Stein, T. Atzet, P. Hays, and M. Tehan, 2004. Effectiveness Monitoring for the Aquatic and Riparian Component of the Northwest Forest Plan: Conceptual Framework and Options. USDA Forest Service General Technical Report PNW-GTR-577, Pacific Northwest Research Station, Portland, Oregon, 71 pp.

Robison, G.E., K.A. Mills, J. Paul, L. Dent, and A. Skaugset, 1999. Storm Impacts and Landslides of 1996: Final Report. Oregon Department of Forestry, Salem, Oregon, 145 pp.

Roni, P., 2002. Habitat Use by Fishes and Pacific Giant Salamanders in Small Western Oregon and Washington Streams. Transactions of the American Fisheries Society 131:743-761.

Sheer, M.B. and E.A. Steel, 2006. Lost Watersheds: Barriers, Aquatic Habitat Connectivity, and Salmon Persistence in the Willamette and Lower Columbia River Basins. Transactions of the American Fisheries Society 135:1645-1669.

Spies, T.A., K.N. Johnson, K.M. Burnett, J.L. Ohmann, B.C. McComb, G.H. Reeves, P. Bettinger, J.D. Kline, and B. Garber-Yonts, 2007. Cumulative Ecological and Socioeconomic Effects of Forest Policies in Coastal Oregon. Ecological Applications 17:5-17.

Stevens, D.L., Jr, and A.R. Olsen, 1999. Spatially Restricted Surveys Over Time for Aquatic Resources. Journal of Agricultural, Biological, and Environmental Statistics 4(4):415-428.

Stock, J.D. and W.E. Dietrich, 2006. Erosion of Steepland Valleys by Debris Flows. Geological Society of America Bulletin 118:1125-1148.

Stoddard, J.L., D.V. Peck, S.G. Paulsen, J. Van Sickle, C.P. Hawkins, A.T. Herlihy, R.M. Hughes, P.R. Kaufmann, D.P. Larsen, G. Lomnicky, A.R. Olsen, S.A. Peterson, P.L. Ringold, and T.R. Whittier, 2005. An Ecological Assessment of Western Stream and Rivers. EPA 620/R-05/005. U.S. Environmental Protection Agency, Washington, D.C.

Tarboton, D.G., 1997. A New Method for the Determination of Flow Directions and Upslope Areas in Grid Digital Elevation Models. Water Resources Research 33:309-319.

Underwood, J. and R.E. Crystal, 2002. Hydrologically Enhanced, High-Resolution DEMs. A Supplement to Geospatial Solutions, April 1, 2002: 8-14. http://www.geospatial-online.com, *accessed* April 2007.

USDA and USDI, 1994. Record of Decision for Amendments to Forest Service and Bureau of Land Management Planning Documents Within the Range of the Northern Spotted Owl. Portland, Oregon [Plus Attachment A: Standards and Guidelines].

USGS (U.S. Geological Survey), 1998. National Mapping Program Technical Instructions: Standards for Digital Elevation Models. U.S. Geological Survey, National Mapping Division. http://rockyweb.cr.usgs.gov/public/nmpstds/demstds.html, *accessed* May 2006.

USGS (U.S. Geological Survey), 2000. The National Hydrography Dataset: Concept and Contents. http://nhd.usgs.gov/, *accessed* July 2006.

Walker, G.W. and N.S. MacLeod, 1991. Geologic Map of Oregon. U.S. Geological Survey, Reston, Virginia, 1:500,000, Lambert Conformal Conic Projection, Colored, 2 Sheets.

Water and Climate Center of the Natural Resources Conservation Service 1998. Western U.S. Average Monthly or Annual Precipitation, 1961-1990. http://www.ocs.orst.edu/prism/products/, *accessed* in June 2006.

Wohl, E. and D. Merrit, 2005. Prediction of Mountain Stream Morphology. Water Resources Research 41, W08419, doi: 10.1029/2004SR003779.

Wondzell, S.M., M.A. Hemstrom, and P.A. Bisson, 2007. Simulating Riparian Vegetation and Aquatic Habitat Dynamics in Response to Natural and Anthropogenic Disturbance Regimes in the Upper Grande Ronde River, Oregon, USA. Landscape and Urban Planning 80:249-267.

Wyatt, R.J., 2003. Mapping the Abundance of Riverine Fish Populations: Integrating Hierarchical Bayesian Models With a Geographic Information System (GIS). Canadian Journal of Fisheries and Aquatic Sciences 60:997-1006.

Young, K., 2000. Riparian Zone Management in the Pacific Northwest: Who's Cutting What? Environmental Management 26:131-144.